International Journal Software Engineering and Computer Science (IJSECS)
6 (2), 2026, 465-473
Published Online August 2026 in IJSECS (http://www.journal.lembagakita.com/index.php/ijsecs)
P-ISSN: 2776-4869, E-ISSN: 2776-3242. DOI: https://doi.org/10.35870/ijsecs.v6i2.7268.

RESEARCH ARTICLE Open Access

Predicting Peak Ground Acceleration Using RNN and LSTM Model on MCGuire's Empirical Calculation

Irna Purwanti [1*], **Taswanda Taryo** [2], **Ferhat Aziz** [3]

[1*] Master of Informatics Engineering, Universitas Pamulang, South Tangerang City, Banten Province, Indonesia.
[2,3] Department of Informatics Engineering, Universitas Pamulang, South Tangerang City, Banten Province, Indonesia.

**Corresponding author*: irna.purwanti@bmkg.go.id.

Received: May 20, 2026; Accepted: June 1, 2026; Published: August 1, 2026.

Abstract: Peak ground acceleration (PGA) is an important parameter in seismic hazard assessment because it represents the maximum ground acceleration generated by an earthquake and informs structural design and disaster mitigation. Predicting PGA remains challenging because seismic-wave propagation is nonlinear and affected by geological heterogeneity. This study developed, evaluated, and spatially mapped recurrent neural network (RNN) and long short-term memory (LSTM) models for predicting PGA values calculated using the McGuire empirical equation in BMKG Regional II, Indonesia, which extends from South Sumatra to West Java. A historical earthquake catalog covering 1971–2025 was used to generate a spatial dataset comprising 3,727 grid points based on surface-wave magnitude and hypocentral distance. The dataset was divided sequentially into 70% training data and 30% testing data. On the test set, the LSTM produced an RMSE of 55.1559, an MAE of 31.0443, and an R^2 of 0.7112, whereas the RNN produced an RMSE of 56.7773, an MAE of 36.5842, and an R^2 of 0.6940. The spatial results also showed that the LSTM reproduced high PGA values more closely than the RNN, which produced smoother estimates in areas with abrupt PGA variations. Within the dataset and model configuration used in this study, the LSTM therefore provided better predictive performance than the RNN for reconstructing the spatial distribution of McGuire-based PGA. The resulting model may support regional seismic hazard assessment, but validation against observed ground-motion records and the inclusion of local site parameters remain necessary before its use in engineering or regulatory applications.

Keywords: Deep Learning; Long Short-Term Memory; Peak Ground Acceleration; Recurrent Neural Network; Seismic Hazard Assessment.

1. Introduction

Indonesia lies within a tectonically active region influenced by the convergence of the Indo-Australian, Eurasian, and Pacific plates. This setting makes the archipelago highly susceptible to frequent and potentially damaging earthquakes (Aldian *et al.*, 2020; Supendi *et al.*, 2022). The area administered by the Agency for Meteorology, Climatology, and Geophysics (BMKG) Regional II extends from South Sumatra to West Java and includes densely populated and economically important areas. Seismicity in this region is influenced by major tectonic systems, including the Sunda Megathrust and the Great Sumatran Fault, which contribute to its earthquake hazard (BMKG, 2024; Natawidjaja, 2021). Assessing ground-motion intensity is therefore important for seismic hazard analysis, infrastructure planning, and earthquake-risk mitigation.

Peak ground acceleration (PGA) represents the maximum absolute ground acceleration recorded during an earthquake. It is commonly used in seismic hazard assessment and structural engineering because ground acceleration is related to the inertial forces imposed on structures during seismic events (Irsyam *et al.*, 2020; Kramer, 1996). PGA is often estimated using deterministic or probabilistic ground-motion prediction equations (GMPEs), also known as attenuation relationships. The McGuire empirical equation estimates PGA as a function of earthquake magnitude and the distance between the earthquake source and the site of interest (Douglas, 2021; McGuire, 1974). Although empirical equations provide a practical basis for regional hazard assessment, their generalized functional forms may not fully represent variations associated with seismic-wave propagation, geological heterogeneity, rupture directivity, and fault mechanisms (Cremen & Galasso, 2020; Wang *et al.*, 2023).

Data-driven approaches have increasingly been applied to model nonlinear relationships that may not be fully represented by conventional empirical equations. Artificial intelligence and machine learning, particularly deep learning, have consequently been adopted in several seismological applications (Kavianpour *et al.*, 2023; Kong *et al.*, 2019). Deep learning models can identify nonlinear patterns in multidimensional datasets without requiring all relationships among the variables to be specified in advance (Bergen *et al.*, 2019; Mahmoud *et al.*, 2023). Many existing deep learning studies on PGA prediction use continuous seismic waveforms. Although waveform-based methods can provide detailed ground-motion information, their implementation depends on the availability and continuity of seismic records and may require substantial computational resources (Priyanto *et al.*, 2023; Zheng *et al.*, 2025). The application of sequence-based models to spatially ordered PGA values derived from empirical equations has received comparatively limited attention. In particular, further evaluation is needed to determine how recurrent neural networks (RNNs) and long short-term memory (LSTM) networks perform when applied to a spatial sequence of grid-based PGA values (Jozinović *et al.*, 2022; Mousavi & Beroza, 2020).

This study developed and compared RNN and LSTM models for predicting the spatial distribution of PGA values calculated using the McGuire empirical equation in BMKG Regional II. The study generated a grid-based PGA dataset, trained the models using spatially ordered coordinate data, evaluated their predictive performance using statistical error metrics, and mapped the predicted values to examine their ability to reproduce areas with relatively high PGA. By combining an empirical PGA equation with recurrent neural networks, this study evaluates a data-driven approach to reconstructing McGuire-based PGA patterns for regional seismic hazard assessment.

2. Related Work

Ground-motion prediction equations (GMPEs) have long provided a basis for estimating peak ground acceleration (PGA) and other ground-motion parameters. Models developed by McGuire (1974), Boore *et al.* (2014), and Campbell and Bozorgnia (2014), for example, estimate ground motion using variables such as earthquake magnitude, source-to-site distance, and site conditions. Despite their widespread use, GMPEs retain residual variability associated with source, path, and site effects, particularly when applied outside the regions or conditions represented by their calibration data (Douglas, 2021). This limitation is relevant to Indonesia, where seismic hazard assessment must account for complex tectonic settings and multiple fault systems (Irsyam *et al.*, 2020). Data-driven methods have therefore been applied to model nonlinear relationships between earthquake parameters and ground motion. Alavi and Gandomi (2011) reported that neural-network-based models could represent complex relationships among ground-motion variables and produce lower prediction errors than the regression methods evaluated in their study. Recurrent architectures have also been investigated because of their ability to process sequential dependencies. Fayaz *et al.* (2021), for instance, developed a hybrid recurrent neural network for ground-motion prediction and compared its performance with alternative modeling approaches.

Long short-term memory (LSTM) networks extend standard recurrent neural networks (RNNs) through gated memory cells that help mitigate the vanishing-gradient problem and retain information across longer sequences. Wang *et al.* (2023) applied an LSTM model to PGA prediction in an earthquake early warning setting using information available after P-wave detection, while Kavianpour *et al.* (2023) combined convolutional neural networks with bidirectional LSTM layers to model earthquake-related parameters. Other studies have focused on real-time prediction and rapid ground-shaking mapping. Mahmoud *et al.* (2023) developed a deep learning model for PGA prediction using strong-motion data, whereas Zheng *et al.* (2025) used records from the K-NET and KiK-net networks to evaluate PGA prediction under varying site conditions. Jozinović *et al.* (2022) applied deep neural networks to raw waveform data to generate rapid estimates of ground-shaking intensity. These studies demonstrate the potential of deep learning for processing sequential seismic information, although their input data, prediction targets, and evaluation procedures differ from those used in spatial PGA modeling. Waveform-based methods also generally depend on the availability, quality, and continuity of instrumental records.

Data-driven PGA modeling has also been examined in Indonesia. Priyanto *et al.* (2023) applied multivariate adaptive regression splines to earthquake data and evaluated magnitude, distance, and source depth as predictors of PGA. Rahmawan *et al.* (2024) used an artificial neural network to estimate PGA in Java, providing a regional example of nonlinear ground-motion modeling. Chasanah *et al.* (2022) mapped earthquake risk levels in East Java using multievent earthquake data, while Aldian *et al.* (2020) discussed the need to update seismic hazard information in Sumatra using recent active-fault parameters. These studies indicate increasing use of statistical and machine-learning methods in regional seismic assessment, but they differ in their data structures, target variables, geographic coverage, and validation procedures.

Most deep learning studies reviewed here used seismic waveforms or conventional tabular earthquake data. The application of recurrent models to spatially ordered grid data generated using an empirical PGA equation has received comparatively limited attention. Direct comparisons between standard RNN and LSTM architectures under the same training and testing configuration also remain limited for this type of dataset. The present study addresses this issue by comparing RNN and LSTM models trained on spatially ordered PGA values calculated using the McGuire equation. The comparison evaluates whether the LSTM can reproduce high-gradient variations in the McGuire-based PGA surface more accurately than the standard RNN within the study area and experimental configuration.

3. Methodology

3.1 Study Area and Dataset Preparation

The study area covered BMKG Regional II, extending from South Sumatra to West Java and including the Sunda Strait. Its spatial boundaries ranged from 2°S to 8°S and from 100°E to 110°E. The region is influenced by the subduction of the Indo-Australian Plate beneath the Eurasian Plate and by crustal fault systems that generate frequent seismic activity. Historical earthquake records covering 1971–2025 were obtained from the United States Geological Survey (USGS) and BMKG catalogs. The initial dataset contained approximately 12,000 seismic events. Events with a surface-wave magnitude below 4.0 were excluded, and a spatial grid containing 3,727 coordinate points was generated across the study area.

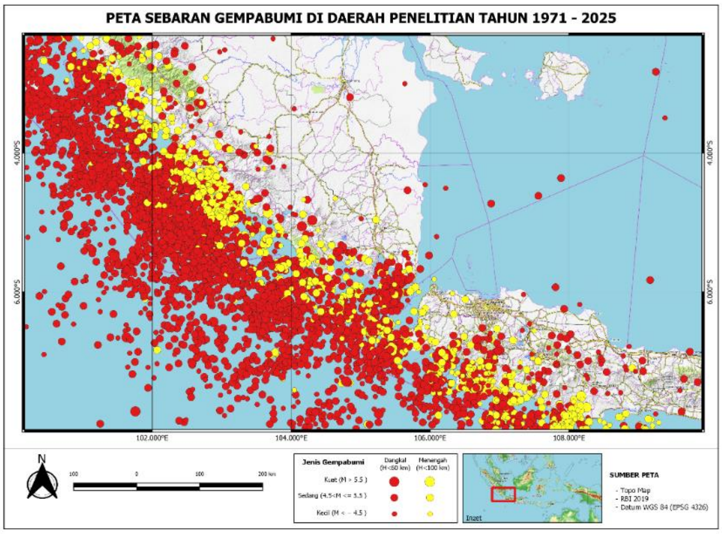

Figure 1. Seismotectonic Map of the Study Area

Figure 1 shows the distribution of historical earthquake epicenters within and around the study area. Earthquake clusters are visible along the western coast of Sumatra and the southern coast of Java, corresponding to seismic activity associated with the Sunda subduction zone. Shallow crustal seismicity is also distributed along Sumatra, including areas influenced by the Great Sumatran Fault. The spatial distribution illustrates the heterogeneous seismic setting of BMKG Regional II and provides the geographical context for calculating grid-based PGA values.

3.2 McGuire PGA Calculation

The maximum peak ground acceleration (PGA) at each of the 3,727 grid points was calculated using the McGuire empirical equation (McGuire, 1974). For each earthquake–grid-point pair, the source-to-site distance was calculated from the geographic coordinates using the Haversine formula, which accounts for Earth's curvature. The McGuire equation was then applied as follows:

$$\mathrm{PGA} = \frac{472.3 \times 10^{0.278 M_s}}{(r + 25)^{1.301}}$$

Where PGA is expressed in Gal, equivalent to cm/s²; M_s denotes surface-wave magnitude; and r denotes the source-to-site distance in kilometers. The equation was applied to the earthquake records at each grid point, and the maximum calculated PGA was retained as the target value for that coordinate. The PGA values were subsequently normalized to the range of 0–1 using MinMaxScaler before model training.

Table 1. Sample of PGA Values Calculated Using the McGuire Equation

Latitude (°)	Longitude (°)	PGA (Gal)
−2.250	100.000	281.5607
−2.375	100.000	421.2788
−2.500	100.000	607.4280
−2.625	100.000	380.9086
−2.750	100.000	260.9524
−2.875	100.000	225.0315
−3.000	100.000	232.9815
−3.125	100.000	297.2304
−3.250	100.000	398.6637
−3.375	100.000	565.4094
−3.500	100.000	702.4254
−3.625	100.000	524.2943
−3.750	100.000	373.2484
−3.875	100.000	281.5247
−4.000	100.000	222.5901
−4.125	100.000	182.2264
−4.250	100.000	153.1382
−4.375	100.000	131.3262
−4.500	100.000	114.4475
−4.625	100.000	101.0501
−4.750	100.000	90.1915
−4.875	100.000	84.2476
−5.000	100.000	83.6856
−5.125	100.000	81.1156

Table 1 presents a subset of the spatial PGA dataset at longitude 100°E. The variation among adjacent grid points reflects differences in the maximum PGA values calculated from the earthquake catalog using the magnitude–distance relationship in the McGuire equation. Because the equation uses magnitude and source-to-site distance, the resulting baseline does not explicitly represent local site amplification associated with near-surface geology or soil conditions. In the deep learning models, latitude and longitude were used as spatial input features, while the calculated PGA served as the prediction target.

3.3 Deep Learning Architecture

Two recurrent architectures were developed and evaluated: a standard recurrent neural network (RNN) and a long short-term memory (LSTM) network. Although these architectures are commonly used for temporal sequences, they were applied in this study to a spatially ordered sequence of grid points. The two-dimensional coordinate grid was flattened through lexicographical sorting. The points were ordered row by row, from west to east in ascending longitude and from north to south in descending latitude. This procedure established a consistent sequence through the grid while preserving proximity among points within each row. A standard RNN transfers its hidden state from one sequence step to the next, enabling information from preceding inputs to influence subsequent predictions. However, standard RNNs can experience vanishing gradients during backpropagation, which may limit their ability to retain information across long sequences. An LSTM uses a memory cell regulated by forget, input, and output gates. These gates control the retention, addition, and transmission of information through the sequence and can improve the model's ability to represent longer-range dependencies.

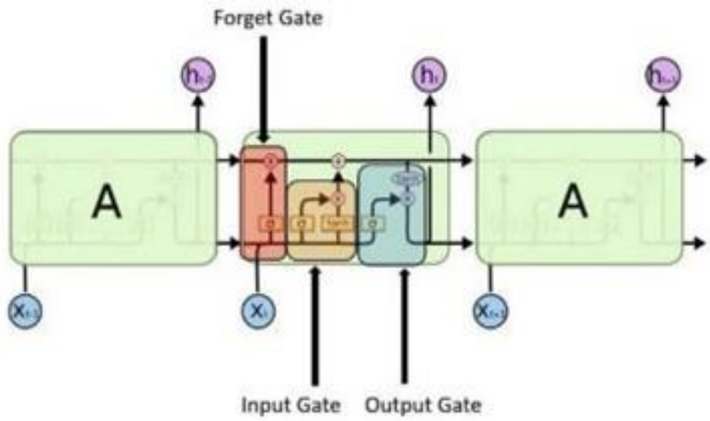

Figure 2. LSTM Architecture Used for Spatial PGA Modeling

Figure 2 illustrates the information flow within the LSTM architecture. At each sequence step, the current coordinate input is processed together with the previous hidden and cell states. Sigmoid and hyperbolic tangent functions regulate the information passed through the gates and memory cell. In this study, this recurrent mechanism was used to model dependencies among spatially ordered grid points rather than temporal observations. The dataset was divided sequentially into 70% training data and 30% testing data. Both models were trained using the same selected hyperparameter values, as summarized in Table 2, to provide a consistent basis for comparison.

Table 2. Hyperparameter Configuration of the RNN and LSTM Models

Parameter	RNN	LSTM
Recurrent layers	1	1
Units	50	50
Activation function	tanh	tanh
Optimizer	Adam	Adam
Loss function	MSE	MSE
Training epochs	100	100
Batch size	32	32

Both models consisted of one recurrent layer with 50 units and used the hyperbolic tangent activation function. The Adam optimizer minimized the mean squared error (MSE) loss over 100 training epochs with a batch size of 32. Using the same selected values for the principal training hyperparameters provided a controlled basis for comparing the models, although the internal gating structure of the LSTM resulted in a different number of trainable parameters from that of the standard RNN.

3.4 Evaluation Metrics

Model performance on the testing subset was evaluated using root mean squared error (RMSE), mean absolute error (MAE), and the coefficient of determination (R^2). MAE represents the average absolute difference between the target and predicted values. RMSE assigns greater weight to large prediction errors because the residuals are squared before averaging. R^2 measures the proportion of variation in the target values represented by the predictions. The metrics were calculated as follows:

$$\mathrm{MAE} = \frac{1}{n}\sum_{i=1}^{n}|y_i - \hat{y}_i|$$

$$\mathrm{RMSE} = \sqrt{\frac{1}{n}\sum_{i=1}^{n}(y_i - \hat{y}_i)^2}$$

$$R^2 = 1 - \frac{\sum_{i=1}^{n}(y_i - \hat{y}_i)^2}{\sum_{i=1}^{n}(y_i - \bar{y})^2}$$

In these equations, $y_i$denotes the target PGA value, $\hat{y}_i$denotes the predicted PGA value, $\bar{y}$is the mean of the target values, and $n$is the number of observations in the testing subset. RMSE was used to evaluate the models' sensitivity to relatively large prediction errors, while MAE provided an error measure that was less strongly influenced by extreme residuals.

4. Result and Discussion

4.1 Results

The predictive performance of the RNN and LSTM models was evaluated on the 30% testing subset using RMSE, MAE, and R^2. As shown in Figure 3, the LSTM produced an RMSE of 55.1559 and an MAE of 31.0443, whereas the RNN produced an RMSE of 56.7773 and an MAE of 36.5842. The LSTM also achieved an R^2 of 0.7112, compared with 0.6940 for the RNN. Under the dataset division and model configuration used in this study, the LSTM therefore produced lower prediction errors and represented a larger proportion of the variation in the McGuire-based PGA values.

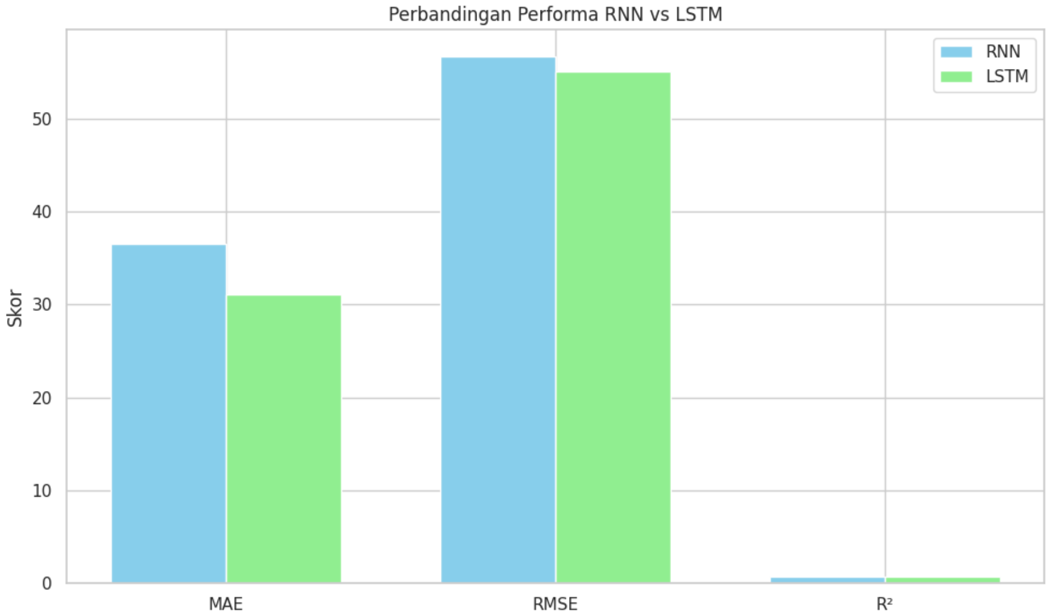

Figure 3. Predictive Performance of the RNN and LSTM Models

The spatial distributions of the McGuire-based reference values and the predictions generated by the two models are presented in Figure 4. The reference surface contained abrupt variations in PGA, including a peak of 698.65 Gal near 3.5°S [cek data: tambahkan bujur dan verifikasi nilainya dengan Table 1]. At the corresponding coordinate, the RNN predicted 603.24 Gal, whereas the LSTM predicted 693.28 Gal. The RNN output appeared smoother around this high-PGA location, while the LSTM prediction was closer to the corresponding McGuire-based value. Similar spatial comparisons should be interpreted using a common color scale across all panels.

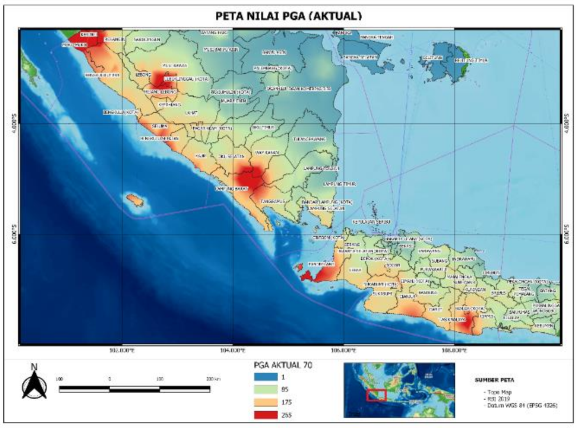

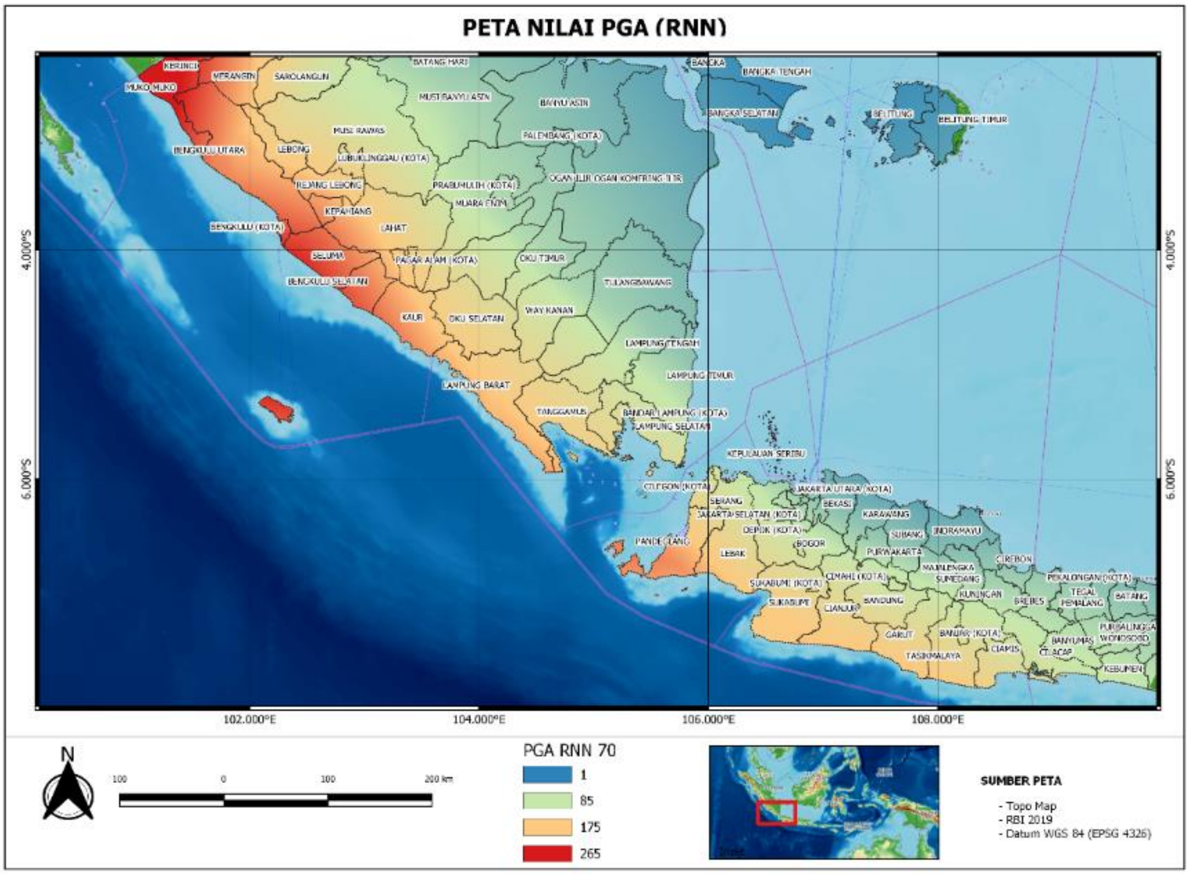

Figure 4. Spatial Distribution of McGuire-Based PGA and the RNN and LSTM Predictions

4.2 Discussion

The quantitative results indicate that the LSTM performed better than the standard RNN under the experimental configuration used in this study. The difference was more pronounced for MAE than for RMSE: the MAE decreased from 36.5842 for the RNN to 31.0443 for the LSTM, while the RMSE decreased from 56.7773 to 55.1559. The higher R^2 obtained by the LSTM likewise indicates that its predictions more closely represented the variation in the testing targets. These results are limited to a single dataset partition and the selected hyperparameter configuration; without repeated training runs or statistical testing, they do not establish that the performance difference is statistically significant. The spatial comparison provides additional information about the models' behavior around areas with abrupt changes in the McGuire-based PGA surface. At the reported peak location, the RNN underestimated the reference value by a larger margin than the LSTM. The gated memory mechanism of the LSTM may have contributed to its ability to retain information across the ordered grid sequence, whereas the standard RNN produced a smoother estimate at this location. This explanation remains interpretive because the study did not directly examine gradient behavior, hidden-state representations, or the effects of sequence length. Moreover, the recurrent sequence was constructed by sorting grid coordinates rather than from a physical time series, so the observed differences should be understood as performance on a spatially ordered dataset rather than evidence that the model learned fault-rupture dynamics. Previous regional studies have used multivariate adaptive regression splines and feed-forward neural networks for PGA modeling (Priyanto *et al.*, 2023; Rahmawan *et al.*, 2024). These studies provide relevant methodological context, but their results cannot be compared directly with the present findings because they used different datasets, input structures, and evaluation procedures.

Although the LSTM achieved an R^2 of 0.7112, a portion of the variation in the McGuire-based target values remained unexplained. This residual variation may reflect the model architecture, spatial sequence construction, training configuration, dataset partition, and optimization procedure. It should not be attributed solely to the absence of geotechnical variables because the target values were themselves calculated using the magnitude–distance relationship in the McGuire equation. Nevertheless, the absence of local site parameters—including time-averaged shear-wave velocity in the upper 30 m, soil classification, and basin characteristics—limits the physical interpretation and practical application of the resulting PGA maps. These variables can influence observed ground motion but were not represented in either the input features or the empirical target. Consequently, the results demonstrate the models' ability to reconstruct a McGuire-based PGA surface rather than their accuracy in predicting observed site-specific ground motion. Validation against instrumental ground-motion records and the inclusion of relevant site parameters would therefore be required before the model could be considered for engineering design or regulatory hazard assessment.

5. Conclusion and Recommendations

This study developed and compared recurrent neural network (RNN) and long short-term memory (LSTM) models for predicting the spatial distribution of peak ground acceleration (PGA) values calculated using the McGuire empirical equation in BMKG Regional II. Under the dataset partition and model configuration used in this study, the LSTM produced better predictive performance than the standard RNN. The LSTM achieved an RMSE of 55.1559 and an R^2 of 0.7112, whereas the RNN produced an RMSE of 56.7773 and an R^2 of 0.6940. The spatial comparison also showed that the LSTM reproduced the reported high-PGA location more closely, while the RNN generated a smoother estimate around the same location. These results indicate that the LSTM was more effective than the RNN in reconstructing the spatially ordered McGuire-based PGA surface examined in this study. However, the findings should not be interpreted as validation against observed ground motion because both models were trained and tested using target values generated from the same empirical equation.

The current model used spatial coordinates as input features and did not explicitly incorporate local geological and geotechnical conditions. Future research should validate model predictions against instrumental ground-motion records and evaluate the effects of including site-related variables, such as time-averaged shear-wave velocity in the upper 30 m (Vs30), soil classification, basin characteristics, and topographic slope. Alternative architectures, including convolutional neural network–LSTM models, could also be examined for spatial feature extraction and sequence modeling, provided that their performance is assessed using the same dataset and validation procedure. Spatial or temporal cross-validation, repeated training runs, and comparisons with nonrecurrent baseline models would provide a stronger assessment of model generalizability. These extensions are necessary before the resulting PGA maps can be considered for site-specific seismic assessment, engineering design, or regulatory applications.

References

Alavi, A. H., & Gandomi, A. M. (2011). Prediction of principal ground-motion parameters using a hybrid method coupling artificial neural networks and simulated annealing. *Computers & Structures, 89*(23–24), 2176–2194. https://doi.org/10.1016/j.compstruc.2011.08.019

Aldian, F., Sengara, W., & Irsyam, M. (2020). Updating seismic hazard maps of Sumatra, Indonesia based on recent active fault parameters. *IOP Conference Series: Earth and Environmental Science, 417*(1), Article 012015.

Badan Meteorologi, Klimatologi, dan Geofisika. (2024). *Laporan tahunan mitigasi gempabumi dan tsunami Wilayah Regional II*.

Bergen, K. J., Johnson, P. A., de Hoop, M. V., & Beroza, G. C. (2019). Machine learning for data-driven discovery in solid Earth geoscience. *Science, 363*(6433), Article eaau0323. https://doi.org/10.1126/science.aau0323

Boore, D. M., Stewart, J. P., Seyhan, E., & Atkinson, G. M. (2014). NGA-West2 equations for predicting PGA, PGV, and 5% damped PSA for shallow crustal earthquakes. *Earthquake Spectra, 30*(3), 1057–1085. https://doi.org/10.1193/070113EQS184M

Campbell, K. W., & Bozorgnia, Y. (2014). NGA-West2 ground motion model for the average horizontal components of PGA, PGV, and 5% damped linear acceleration response spectra. *Earthquake Spectra, 30*(3), 1087–1115. https://doi.org/10.1193/062913EQS175M

Chasanah, U., Handoyo, E., Rahmawati, N. N., & Musfiana, M. (2022). Mapping risk level based on peak ground acceleration (PGA) and earthquake intensity using multievent earthquake data in Malang Regency, East Java, Indonesia. *Jurnal Ilmu Fisika, 14*(1), 64–72. https://doi.org/10.25077/jif.14.1.64-72.2022

Cremen, G., & Galasso, C. (2020). Earthquake early warning: Recent advances and perspectives. *Earth-Science Reviews, 205*, Article 103184. https://doi.org/10.1016/j.earscirev.2020.103184

Douglas, J. (2022). *Ground motion prediction equations 1964–2021* [Technical report]. University of Strathclyde.

Fayaz, J., Xiang, Y., & Zareian, F. (2021). Generalized ground motion prediction model using hybrid recurrent neural network. *Earthquake Engineering & Structural Dynamics, 50*(6), 1539–1561. https://doi.org/10.1002/eqe.3410

Irsyam, M., Cummins, P. R., Asrurifak, M., Faizal, L., Natawidjaja, D. H., Widiyantoro, S., Meilano, I., Triyoso, W., Rudiyanto, A., Hidayati, S., Ridwan, M., Hanifa, N. R., & Syahbana, A. J. (2020). Development of the 2017 national seismic hazard maps of Indonesia. *Earthquake Spectra, 36*(1_suppl), 112–136. https://doi.org/10.1177/8755293020951206

Jozinović, D., Lomax, A., Štajduhar, I., & Michelini, A. (2021). Erratum: Rapid prediction of earthquake ground shaking intensity using raw waveform data and a convolutional neural network. *Geophysical Journal International, 226*(2), 1249. https://doi.org/10.1093/gji/ggab175

Kavianpour, P., Kavianpour, M., Jahani, E., & Ramezani, A. (2023). A CNN-BiLSTM model with attention mechanism for earthquake prediction. *The Journal of Supercomputing, 79*(17), 19194–19226. https://doi.org/10.1007/s11227-023-05369-y

Kong, Q., Allen, R. M., Schreier, L., & Kwon, Y.-W. (2016). MyShake: A smartphone seismic network for earthquake early warning and beyond. *Science Advances, 2*(2), Article e1501055. https://doi.org/10.1126/sciadv.1501055

Kramer, S. L. (1996). *Geotechnical earthquake engineering*. Prentice Hall.

Mahmoud, M. M., Saad, O. M., Keshk, A., & Ahmed, H. (2023). Prediction model for peak ground acceleration using deep learning. *International Journal of Computers and Information, 10*(3), 175–183. https://doi.org/10.21608/ijci.2023.236143.1131

McGuire, R. K. (1974). *Seismic structural response risk analysis, incorporating peak response regressions on earthquake magnitude and distance* (Report No. R74-51). Massachusetts Institute of Technology, Department of Civil Engineering.

Mousavi, S. M., & Beroza, G. C. (2020). A machine-learning approach for earthquake magnitude estimation. *Geophysical Research Letters, 47*(1), Article e2019GL085976. https://doi.org/10.1029/2019GL085976

Natawidjaja, D. H. (2021). Neotectonics of the Sumatran Fault and paleoseismology of the Mentawai fault. *Journal of Asian Earth Sciences, 214*, Article 104764.

Priyanto, D., Triwijoyo, B. K., Jollyta, D., Hairani, H., & Dasriani, N. G. A. (2023). Data mining earthquake prediction with multivariate adaptive regression splines and peak ground acceleration. *MATRIK: Jurnal Manajemen, Teknik Informatika dan Rekayasa Komputer, 22*(3), 583–592. https://doi.org/10.30812/matrik.v22i3.3061

Rahmawan, S. H., Crysdian, C., & Harini, S. (2024). Prediction of peak ground acceleration (PGA) in Java using artificial neural network method. *International Journal of Informatics and Computation, 6*(2), 44–55. https://doi.org/10.35842/ijicom.v6i2.90

Supendi, P., Nugraha, A. D., Puspito, N. T., & Widiyantoro, S. (2022). Seismicity and fault structures in West Java, Indonesia, from BMKG earthquake catalog data. *Geosciences, 12*(1), Article 15.

Wang, A., Li, S., Lu, J., Zhang, H., Wang, B., & Xie, Z. (2023). Prediction of PGA in earthquake early warning using a long short-term memory neural network. *Geophysical Journal International, 234*(1), 12–24. https://doi.org/10.1093/gji/ggad067

Zheng, Z., Lin, B., Wang, S., Jin, X., Liu, H., & Zhou, Y. (2025). Real-time peak ground acceleration prediction via a hybrid deep learning network. *Geophysical Journal International, 241*(1), 628–640. https://doi.org/10.1093/gji/ggaf062.